Tumor and Stem Cell Biology

Cancer Research

miR-214 Coordinates Melanoma Progression by Upregulating ALCAM through TFAP2 and miR-148b Downmodulation

Elisa Penna[1,2], Francesca Orso[1,2,3], Daniela Cimino[1,2,3], Irene Vercellino[1,2], Elena Grassi[1,2], Elena Quaglino[1,2], Emilia Turco[1,2], and Daniela Taverna[1,2,3]

Abstract

Malignant melanoma is one of the most aggressive human cancers, but the mechanisms governing its metastatic dissemination are not fully understood. Upregulation of miR-214 and ALCAM and the loss of TFAP2 expression have been implicated in this process, with TFAP2 a direct target of miR-214. Here, we link miR-214 and ALCAM as well as identify a core role for miR-214 in organizing melanoma metastasis. miR-214 upregulated ALCAM, acting transcriptionally through TFAP2 and also posttranscriptionally through miR-148b (itself controlled by TFAP2), both negative regulators of ALCAM. We also identified several miR-214–mediated prometastatic functions directly promoted by ALCAM. Silencing ALCAM in miR-214–overexpressing melanoma cells reduced cell migration and invasion without affecting growth or anoikis *in vitro*, and it also impaired extravasation and metastasis formation *in vivo*. Conversely, cell migration and extravasation was reduced in miR-214–overexpressing cells by upregulation of either miR-148b or TFAP2. These findings were consistent with patterns of expression of miR-214, ALCAM, and miR-148b in human melanoma specimens. Overall, our results define a pathway involving miR-214, miR-148b, TFAP2, and ALCAM that is critical for establishing distant metastases in melanoma. *Cancer Res; 73(13); 4098–111. ©2013 AACR.*

Introduction

Malignant melanoma represents the fifth most common neoplasia in human and is one of the most invasive, therapy-resistant, and metastatic tumors, with only about 10% survival, 5 years after diagnosis (1). Over the past decades, its incidence has been increasing by 3% to 8% per year in Western countries while mortality has stabilized. Therefore, it is essential to unravel the molecular events that regulate melanoma aggressiveness and metastatic dissemination. Melanoma progresses rapidly through a radial growth phase, confined entirely in the epidermis, followed by a subsequent vertical growth phase, corresponding to the high-risk melanomas, characterized by invasion of the epidermis upper layer, deep infiltration of the dermis and subcutaneous tissues and formation of lymph-nodal, cutaneous, and visceral metastases in a vast majority of cases (2, 3). The transition from the noninvasive to the invasive and metastatic stage is accompanied by specific and well-characterized molecular changes, such as loss of the AP-2 transcription factors (TFAP2) and expression alterations for genes involved in adhesion, angiogenesis, invasion, and survival, including MCAM-MUC-18, ALCAM, E-cadherin, N-cadherin, VEGF, interleukin (IL)-8, matrix metalloproteinase (MMP)-2, and c-KIT (3). Moreover, $BRAF^{V600E}$ oncogenic mutation is one of the earliest and common molecular events that characterize malignant melanoma (2).

The activated leukocyte cell adhesion molecule, ALCAM/CD166, is a transmembrane glycoprotein, member of the immunoglobulin superfamily, involved in both homotypic and heterotypic (to CD6) cell adhesion (4). ALCAM cis-oligomerization on the cell surface and intercellular interactions synergistically promote network formation at site of cell–cell contacts (5, 6). ALCAM expression is altered in many types of tumors, including melanomas, where it is considered as a prognostic molecular marker for neoplastic progression (7). Indeed, while ALCAM expression is low or absent in nevi, *in situ*, and thin melanomas, ALCAM is detectable in the vertical growth phase melanomas and in metastatic lesions. Significantly, the fraction of ALCAM-positive lesions increases according to invasiveness (Clark level) and thickness (Breslow index) of the melanocytic tumor (8). It was shown that any interference with ALCAM function affects melanoma cell movement and invasion (9, 10) and that ALCAM triggers MMP2 and MMP14 activity (11). However, it is still not known how ALCAM overexpression is induced in melanomas and how it coordinates metastasis formation.

Authors' Affiliations: [1]Molecular Biotechnology Center; [2]Department of Molecular Biotechnology and Health Sciences; and [3]Center for Molecular Systems Biology, University of Torino, Torino, Italy

Note: Supplementary data for this article are available at Cancer Research Online (http://cancerres.aacrjournals.org/).

Corresponding Author: Daniela Taverna, Molecular Biotechnology Center, Department of Molecular Biotechnology and Health Sciences, University of Torino, Via Nizza, 52, 10126, Torino, Italy. Phone: 39-011-670-6497; Fax: 39-011-670-6432; E-mail: daniela.taverna@unito.it

doi: 10.1158/0008-5472.CAN-12-3686

miRNAs (miR) are small endogenous noncoding RNAs that deeply contribute to tumor formation and progression, for their ability to posttranscriptionally downregulate the expression of specific target genes by binding to the 3′-untranslated regions (UTR) of their mRNAs, causing degradation or translation inhibition (12–15). Several miRs, including miR-137, miR-221/222, miR-182, and miR-34a have been found to be involved in melanoma progression by regulating key genes such as *KIT*, *MITF*, *FOXO3*, *ITGB3*, *CCND1*, and *CDKN1B* (16). By using a melanoma progression model (17), consisting of a poorly metastatic human melanoma A375P parental cell line and its highly metastatic variants (MA-2, MC-1), we recently showed that miR-214 coordinates melanoma metastasis dissemination by increasing migration, invasion, extravasation, and survival of melanoma cells. In addition, we identified a pathway coordinated by miR-214 and involving TFAP2A and TFAP2C as well as multiple adhesion molecules, including ALCAM (18). Here, we show that miR-214 mediates ALCAM upregulation by silencing TFAP2 and miR-148b, both negative regulators of ALCAM. More importantly, we present evidences that some miR-214–mediated prometastatic functions are directly exerted by ALCAM.

Materials and Methods

Cell culture

A375P, MA-2, and MC-1 cells were provided by R.O. Hynes (Massachusetts Institute of Technology, Cambridge, MA) and maintained as described previously (17, 18). WK-Mel, SK-Mel-28, and human umbilical vein endothelial cells (HUVEC)-GFP were provided by P. Circosta (Molecular Biotechnology Center, Torino, Italy), L. Poliseno (Core Research Laboratory - Istituto Toscano Tumori, CRL-ITT, Pisa, Italy), and L. Primo (Institute for Cancer Research and Treatment, Candiolo, Italy), respectively and maintained as described (19–21). MDA-MB-231 were from American Type Culture Collection. All the cell lines used were authenticated in the last 6 months by BMR Genomics using the CELL ID System (Promega). $BRAF^{V600E}$ mutation was previously described (21) or assessed by sequencing and pyrosequencing analyses as described in ref. 22. Transient transfections and generation of stable cell lines by lentiviral infections were conducted as described previously (18).

Reagents, antibodies, vectors, primers, RNA, protein, and human melanoma samples analyses

pLemiR-empty and pLemiR-214 expression vectors were described in ref. 18. siALCAM#1 and #2 target 2 different regions within ALCAM coding sequence (starting at positions 1350 and 2123 of ALCAM gene, respectively) and were purchased from QIAGEN (Hs_ALCAM_5 and Hs_ALCAM_6 High Purity-validated siRNAs). pLKO.1-shALCAM lentiviral vector targets a region within ALCAM 3′-UTR (at position 2624 of *ALCAM* gene) and was purchased from Open Biosystems (cat. no. RHS3979). miR precursors and inhibitors and assays for quantitative real-time PCR (qRT-PCR) miR detection were from Applied Biosystems. RNA (miR and mRNA) and protein extraction and detection (qRT-PCR and Western blotting, respectively) were previously described in ref. 18. Luciferase and chromatin immunoprecipitation (ChIP) assays were conducted with the Dual-Luciferase Reporter System (Promega) and the EZ-Magna ChIP G (Millipore) kits, respectively. Melanoma samples were collected from the Institute Dermatologic Clinic of the University of Torino (Torino, Italy) and approvals were obtained for all samples; RNA extraction and analyses were conducted as in ref. 18.

In vitro biologic assays

Migration, invasion, proliferation, anchorage-independent growth, transendothelial migration, and anoikis assays were previously described in ref. 18.

In vivo metastasis assays

All experiments carried out with live animals complied with ethical animal care. For experimental metastasis assays, 5×10^5 MA-2, WK-Mel, and SK-Mel-28 cells were injected into the tail vein of 6- to 8-week-old NOD/SCID/IL2Rγ^{null} (NSG) immunocompromised mice and the animals were dissected 3 (MA-2, SK-Mel-28) or 5 (WK-Mel) weeks later. Spontaneous metastases were evaluated in 6- to 8-week-old NSG mice subcutaneously injected in the back with 5×10^6 MA-2 cells and dissected 7 weeks later. Red fluorescent lung and liver (when present) metastases were evaluated and photographed in fresh total lungs using a Leica MZ16F fluorescence stereomicroscope. The area or the number of metastases was measured on photographs using the ImageJ software (http://rsbweb.nih.gov/ij/). Micrometastases were evaluated with the Panoramic View program on paraffin-embedded and hematoxylin and eosin (H&E)–stained specimens, scanned with Panoramic Desk (3DHistech; Euroclone).

In vivo extravasation assay

A total of 1.5×10^6 MA-2 or WK-Mel cells, previously labeled with CellTracker Orange CMRA (Molecular Probes, Invitrogen Life Technologies), were injected into the tail vein of 7-week-old female CD1 nude mice (Charles River Laboratories). Two or 48 hours later, mice were sacrificed and 4% paraformaldeyde was injected into the trachea. Total lungs were dissected and photographed using a Leica MZ16F fluorescence stereomicroscope and red fluorescent cells were counted 48 hours following injections using the ImageJ software (http://rsbweb.nih.gov/ij/). Lungs were included in freezing resin (OCT Killik, Bio-Optica, IT) and cryostat-cut in 6-μm thick sections. Immunofluorescent stainings for blood vessels were conducted with anti-CD31 primary antibody (1:100 dilution) and specimens examined using a Zeiss AxioObserver microscope with the ApoTome Module (18).

In silico analyses

TFAP2 putative binding sites were obtained by the classical positional weight matrices (PWM) approach (23), as described in ref. 24. TFAP2 matrix was obtained from the JASPAR CORE database and background nucleotide frequencies were derived from the analyzed sequence. We considered high-affinity sites those with a score higher than 80% of the maximum score (i.e., the score of the perfect match for the PWM) and low-affinity sites those less than 80% but more than 60%. To assess direct interactions between miR-214 and miR-148b, we evaluated

2,000 nucleotides upstream and downstream of pre-miR-148b, considering the mean lengths of pri-miRs reported in ref. 25. RNA Hybrid algorithm (26) was used, either with or without the option that forces to obtain a perfect helix in the 2 to 7 region of the seed. The *P* value was estimated using as background either the human intronic dinucleotides frequencies or the default 3′-UTR–based ones. $P > 0.05$ was considered nonstatistically significant. The result was confirmed by LALIGN manual alignment program.

Statistical analyses

Data are presented as mean ± SD or as mean ± SEM, as indicated, and two-tailed Student *t* test was used for comparison, with *, $P < 0.05$; **, $P < 0.01$; ***, $P < 0.001$ considered to be statistically significant. ns indicates a nonstatistically significant *P* value.

All reagents, antibodies, vectors, and primer sequences used in this study, as well as detailed experimental procedures are described in the Supplementary Materials and Methods.

Results

ALCAM is upregulated by miR-214 in melanoma

As summarized in Supplementary Table S1, here and previously (18), we proved that the ability of miR-214 to promote cell movement and metastasis formation *in vitro* is independent of $BRAF^{V600E}$ mutation status as for various melanoma cell lines analyzed. Interestingly, when miR-214 was overexpressed both in a transient (pre-miR-214, 48 and 72 hours posttransfection) or stable (pLemiR-214) manner in the $BRAF^{V600E}$-mutated A375P, MA-2, and SK-Mel-28 or in the $BRAF^{WT}$ WK-Mel melanoma cell lines (Supplementary Fig. S1A and S1B), a significant ALCAM protein or mRNA upregulation

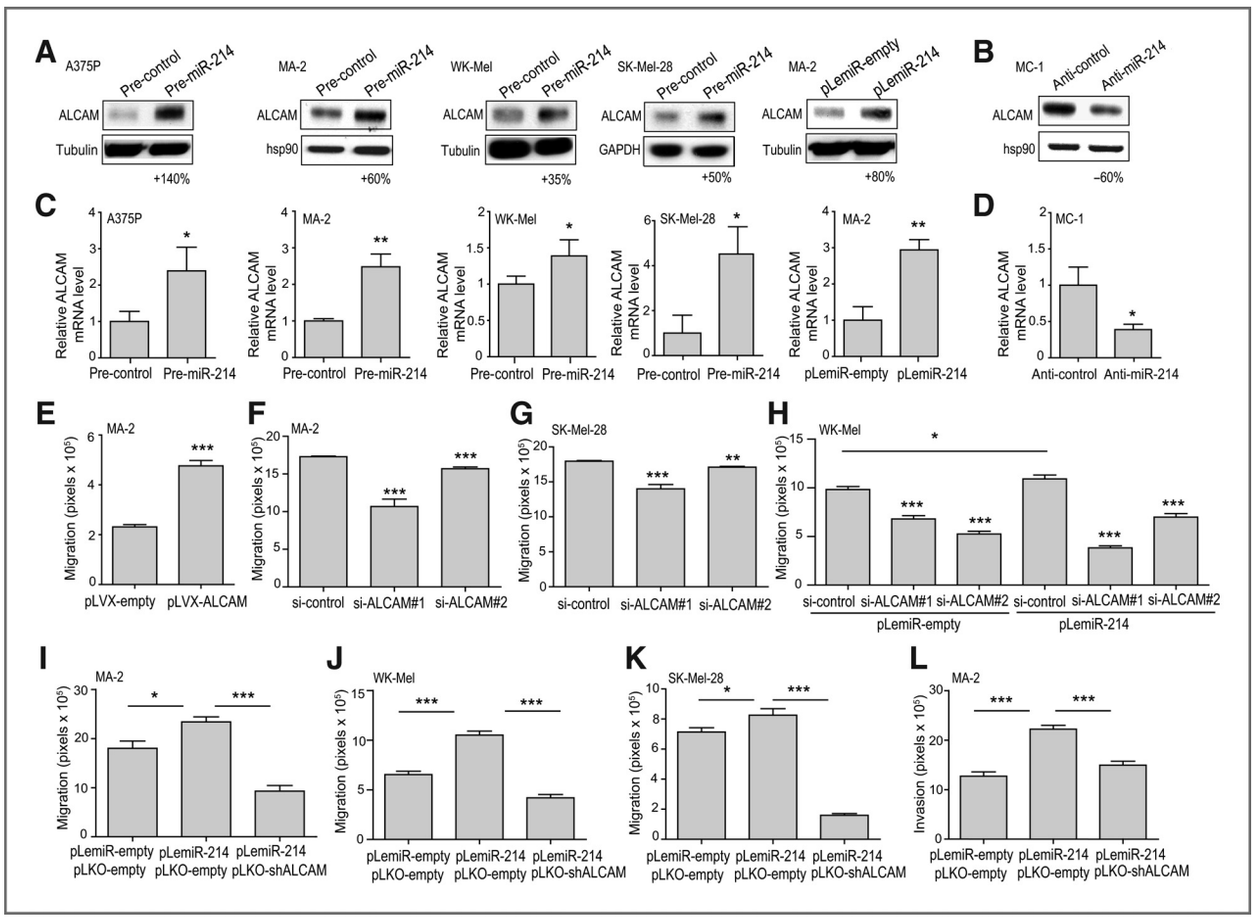

Figure 1. ALCAM is upregulated by miR-214 and controls melanoma cell movement. A and B, Western blot analyses of ALCAM protein levels in the indicated melanoma cell lines after transfections with miR-214 precursors or inhibitors or their negative controls (pre- and anti-miR-214 or -control, 72 or 48 hours posttransfection, respectively) or in MA-2 cells stably transduced with pLemiR-empty or miR-214 overexpression (pLemiR-214) vectors. Protein modulations were calculated relative to controls, normalized on tubulin or hsp90 or GAPDH loading controls, and expressed as percentages. C and D, ALCAM mRNA levels measured by qRT-PCR in the indicated melanoma cells transfected or transduced as in A and B. Results were calculated as fold changes (mean ± SD of triplicates) relative to controls, normalized on 18S RNA level. E–L, Transwell migration (E–K) or Matrigel invasion (L) assays for MA-2, WK-Mel or SK-Mel-28 cells transiently transfected with either pLVX-empty or pLVX-ALCAM overexpression vectors (E), or with either control or ALCAM-targeting siRNAs (si-control or si-ALCAM#1 or #2; F–H), or cotransduced with pLemiR-empty or pLemiR-214 vectors and with either empty or ALCAM-targeting shRNA vectors (pLKO-empty or pLKO-shALCAM; I–L). Results are shown as mean ± SEM of the area covered by migrated cells. At least 2 independent experiments were carried out (in triplicate for C–L) and representative results are shown.

(from +35% to +280%) was observed as shown in Western blot (Fig. 1A and Supplementary Fig. S2A) or qRT-PCR (Fig. 1C) analyses, compared with controls (pre-control or pLemiR-empty), independently of BRAF alterations. Consistently, as shown in Fig. 1B and D, ALCAM expression was decreased (−60%) both at protein and at mRNA level following miR-214 inhibition by anti-miR-214 in transiently transfected MC-1 cells (Supplementary Fig. S1E) compared with controls. Reduced ALCAM expression was also observed in cells expressing miR-214–specific sponges (Orso and colleagues, unpublished data). Relevantly, correlation between miR-214 overexpression and ALCAM upregulation was also observed in other tumor cells, such as the breast cancer MDA-MB-231 cells (Supplementary Figs. S1A and S2A).

ALCAM upregulation controls miR-214–mediated melanoma cell movement, invasion, and metastatic dissemination

To investigate the potential involvement of ALCAM in miR-214 prometastatic functions, we first modulated ALCAM in different melanoma cells to obtain transient overexpression or silencing, using respectively a cDNA-expression vector (pLVX-ALCAM, MA-2 cells) or 2 independent siRNAs (si-ALCAM#1 and #2, MA-2 and SK-Mel-28 cells) and evaluated its biologic relevance compared with control cells (pLVX-empty or si-control, respectively). As shown by Western blot analyses in Supplementary Fig. S1I, relevant ALCAM upregulation or silencing was obtained. These cells were used to evaluate cell growth and migration *in vitro* and, while no effects were observed for serum-dependent proliferation (Supplementary Fig. S2B), a significant enhancement or reduction of cell movement was observed for ALCAM overexpressing (Fig. 1E) or silenced (Fig. 1F and G) cells, compared with controls, thus phenocopying miR-214 expression modulations (18). To assess whether the prometastatic phenotype associated with miR-214 overexpression in melanoma cells could be rescued, at least in part, by ALCAM silencing, we silenced ALCAM in a transient manner by siRNAs (Fig. 1H; WK-Mel cells) or stably (pLKO-shALCAM) in control (pLemiR-empty) or miR-214–overexpressing (pLemiR-214) MA-2, WK-Mel, and SK-Mel-28 cells, compared with controls (si-control or pLKO-empty), as shown in Supplementary Fig. S1I. When we evaluated the biologic properties of these cells *in vitro*, we observed a strong reduction (about 50% decrease) in cell migration or Matrigel invasion following ALCAM silencing in miR-214–overexpressing cells (Fig. 1H–L), whereas no effect on MA-2 serum-dependent proliferation (Supplementary Fig. S2C) or anchorage-independent growth in soft agar (Supplementary Fig. S2D) was found, leading us to conclude that ALCAM is able to rescue miR-214–induced increase in cell movement.

As previously shown for MA-2 cells (18) and in Fig. 2B and C for WK-Mel and SK-Mel-28 cells, miR-214 overexpression (pLemiR-214) induces increased metastatic dissemination *in vivo*, compared with empty controls. To evaluate the role of ALCAM in miR-214–mediated melanoma cell dissemination, miR-214–overexpressing MA-2 (Fig. 2A) or WK-Mel (Fig. 2B) or miR-214–overexpressing SK-Mel-28 (Fig. 2C) cells (pLemiR-empty or pLemiR-214, turbo red fluorescent protein-tRFP–positive), stably silenced (pLKO-shALCAM) or not (pLKO-empty) for ALCAM, were injected in the tail vein of severely immunocompromised NSG mice and metastatic nodules evaluated 3 to 5 weeks postinjections in the lungs (and livers for MA-2 cells). As assessed by the quantitation of metastatic areas in the whole organs (Fig. 2A, a–d) or in H&E-stained sections (Supplementary Fig. S2F, a and b), or by counting metastatic colonies in H&E-stained sections (Fig. 2B, a–d) or in whole lungs (Fig. 2C, a–e), colony formation for ALCAM-silenced melanoma cells was significantly impaired compared with controls and, more importantly, ALCAM silencing in miR-214–overexpressing cells rescued miR-214–driven increased metastasis formation. In addition, spontaneous metastasis formation was evaluated following subcutaneous injection of miR-214–overexpressing ALCAM-silenced MA-2 cells in NSG mice, looking for fluorescent microscopic metastatic lesions 7 weeks later. Primary tumor growth was also evaluated here and no difference was found (Fig. 2D, top). However, as shown in Fig. 2D, bottom, a–c, the increased number of lung micrometastases found for miR-214–overexpressing cells was significantly rescued when ALCAM was silenced. Very few metastatic lesions were observed in the livers.

Because these *in vitro* and *in vivo* results were obtained for 3 distinct melanoma cell lines and independently of $BRAF^{V600E}$ mutation status (Supplementary Table S1), they indicate a general key role for miR-214–mediated ALCAM upregulation in melanoma metastasis. Interestingly, transient ALCAM silencing (si-ALCAM#1) was able to significantly reduce *in vitro* cell movement compared with si-control also in the MDA-MB-231 breast cancer cell line (Supplementary Figs. S1I and S2E), suggesting a broader function for miR-214–driven ALCAM upregulation in tumor cell movement.

ALCAM controls melanoma cell extravasation

To evaluate the possible involvement of ALCAM in tumor cell extravasation, we first analyzed *in vitro* transendothelial migration by seeding CMRA-labeled (red) MA-2 cells previously silenced (si-ALCAM#1) or not (si-control) for ALCAM in the upper chamber of Transwell covered by a confluent HUVECs-GFP monolayer. As shown in Fig. 3A, ALCAM downmodulation (b) decreased transendothelial migration compared with control (a). More relevantly, ALCAM transient (si-ALCAM#1; Supplementary Fig. S2G) or stable (pLKO-shALCAM) downmodulation in miR-214–overexpressing MA-2 cells (pLemiR-214, tRFP-positive) abolished miR-214–mediated enhancement of transendothelial migration (pLemiR-214+pLKO-empty) and reestablished migration levels comparable with controls (pLemiR-empty+pLKO-empty; Fig. 3B, a–c). Transient ALCAM silencing was able to significantly reduce transendothelial migration also in MDA-MB-231 cells (Supplementary Fig. S2H), again suggesting a general role in tumor cell dissemination. We then evaluated ALCAM involvement in *in vivo* extravasation in the lungs of immunocompromised mice following tail vein injections of miR-214–overexpressing MA-2 or WK-Mel cells (pLemiR-214) transduced with either pLKO-shALCAM or pLKO-empty control (Fig. 3C and D). The lodging in lung vasculature was evaluated 2 hours post-injection (a and b) when the cells resulted localized inside or

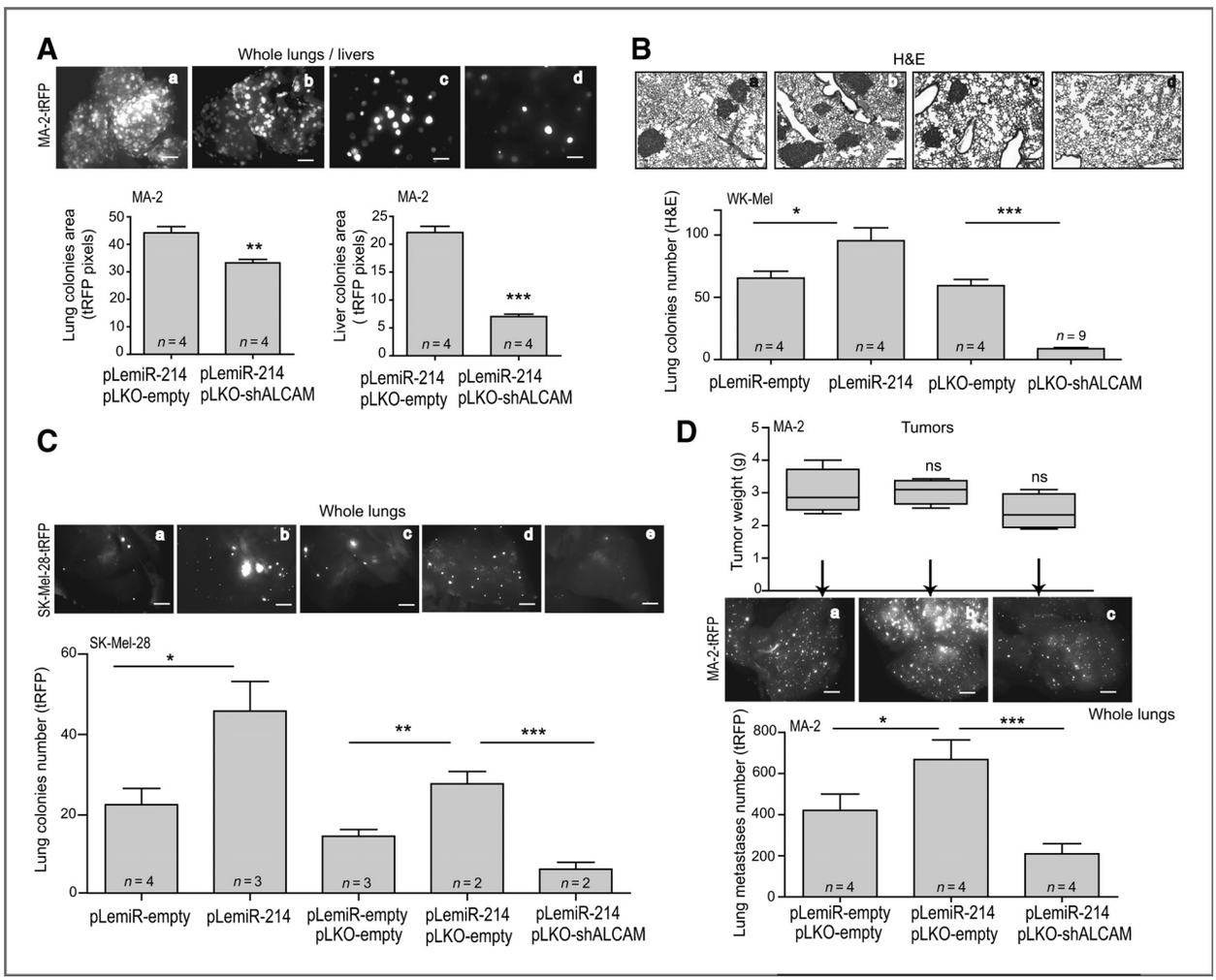

Figure 2. ALCAM upregulation by miR-214 promotes melanoma metastasis formation. A–C, colony formation in lungs (A, left; B and C) or livers (A, right) of NSG mice, 3 or 5 weeks after tail vein injection of MA-2, WK-Mel, or SK-Mel-28 cells, transduced or cotransduced with pLemiR-empty or miR-214 overexpression (pLemiR-214) vectors (expressing tRFP) and/or with either empty or ALCAM-targeting shRNA vectors (pLKO-empty or pLKO-shALCAM). D, NSG mice were subcutaneously injected in the back with MA-2 cells cotransduced with pLemiR-empty or pLemiR-214 vectors (expressing tRFP) and with either pLKO-empty or pLKO-shALCAM vectors and sacrificed 7 weeks later. Primary tumor weights are shown at the top, lung micrometastases at the bottom. Representative pictures of whole lungs and livers (A, a–d, bar, 2 mm; C, a–e; and D, a–c, bar, 800 μm) or of H&E stainings (B, a–d, bar, 200 μm) are shown. Results are indicated as mean ± SEM of the fluorescent area (A) or of the number of lung colonies counted on H&E-stained sections (B) or of the number of fluorescent colonies counted in the whole lungs (C and D, bottom) or as box and whiskers plot for tumor weights (D, top) for the number of mice per group (*n*) indicated in each column. Two independent experiments were carried out for A and B and representative results are shown.

associated with blood vessels, as shown by vessel stainings (Supplementary Fig S2I, a and b), and no difference was observed. Instead, a 50% decrease in early lung colonization at 48 hours postinjection was found following ALCAM silencing compared with controls (c and d). At this time point, the melanoma cells were extravasated and dispersed in the lung parenchyma (Supplementary Fig S2I, c and d). When we tested the possible ALCAM function in cell survival in the absence of adhesion and serum (anoikis), that is a condition resembling the situation of detached invading or intravasated tumor cells, only an irrelevant increase of apoptosis for ALCAM-silenced MA-2 cells (pLKO-shALCAM, Fig. 3E) was observed.

miR-214–driven ALCAM upregulation in melanoma cells partially depends on TFAP2-mediated transcriptional repression

To identify the molecular mechanisms leading to ALCAM upregulation by miR-214, we first considered a possible transcriptional regulation. We previously showed that the transcription factors TFAP2A and TFAP2C are targeted by miR-214 in MA-2 cells (18); we now observed relevant TFAP2A and TFAP2C downmodulation by miR-214 also in WK-Mel and SK-Mel-28 cells (Fig 4A). Thus, we evaluated the possibility of a TFAP2-mediated transcriptional repression on the ALCAM promoter. To test the potential ALCAM transcriptional repression by TFAP2 factors, MA-2 cells were transiently transfected

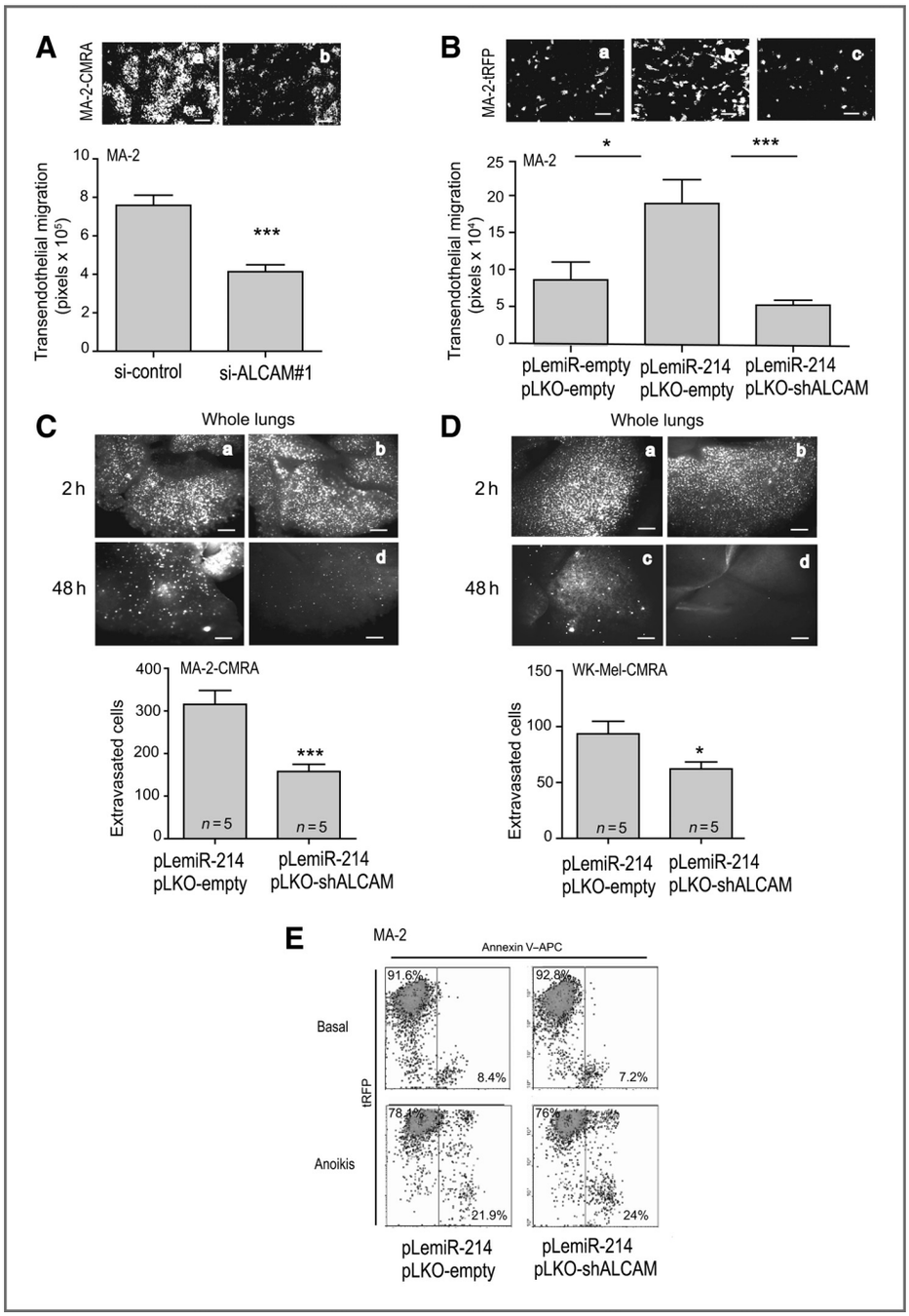

Figure 3. ALCAM controls melanoma cell extravasation. A and B, transendothelial migration assays of CMRA-labeled MA-2 cells transiently transfected with either control or ALCAM-targeting siRNAs (si-control or si-ALCAM#1; A) or of MA-2 cells cotransduced with pLemiR-empty or miR-214 overexpression (pLemiR-214) vectors (expressing tRFP) and with either empty or ALCAM-targeting shRNA vectors (pLKO-empty or pLKO-shALCAM; B), through a fibronectin-coated Transwell membrane covered by a confluent monolayer of HUVECs-GFP. Transmigrated MA-2 cells on the lower side of the Transwell are shown in a–c. Bar, 50 μm. C and D, *in vivo* extravasation assays 2 hours (a and b) or 48 hours (c and d) following tail vein injections in nude mice of MA-2 (C) or WK-Mel (D) cells cotransduced as in B. Representative pictures of whole lungs are shown; bar, 800 μm. E, anoikis assay for MA-2 cells transduced as in C and plated in the absence of adhesion and serum for 72 hours. Cell death percentage was evaluated by Annexin V–allophycocyanin staining, displayed in bidimensional plots. Left quadrant, healthy population; right quadrant, apoptotic population. Two or 3 independent experiments were carried out (in triplicate for A, B, and E) and representative results are shown as mean ± SEM of the area covered by migrated cells (A and B) or of the number of extravasated cells at 48 hours for $n = 5$ mice per group (C and D) or as percentages of cells (E).

with TFAP2A or TFAP2C expression constructs [pSP(RSV)-TFAP2A, pSP(RSV)-TFAP2C], or with the combination of both, or with an empty control [pSP(RSV)-empty] and ALCAM mRNA and protein expression was analyzed by qRT-PCR and Western blot analysis, respectively. As shown in Fig. 4B and C, TFAP2 overexpression resulted in 20% to 40% decreased ALCAM mRNA and protein expression, 48 and 72 hours post-transfection, respectively. A similar ALCAM protein down-modulation following TFAP2 overexpression was observed in WK-Mel cells (Fig. 4D). Consistently, in TFAP2C-silenced cells (pLKO-shTFAP2C), we observed 20% increased ALCAM protein expression compared with control (pLKO-empty), as shown in Fig. 4E. These results suggested that miR-214–driven ALCAM upregulation could depend on TFAP2A and/or TFAP2C decrease due to miR-214 targeting. In line with this, we observed lower ALCAM levels in miR-214–overexpressing (pLemiR-214) MA-2 cells when TFAP2A or, to a lesser extent, TFAP2C [pSP(RSV)-TFAP2A, pSP(RSV)-TFAP2C] or both were overexpressed compared with controls (Fig. 4F). The ALCAM promoter region, from −900 to +100 bp relative to the

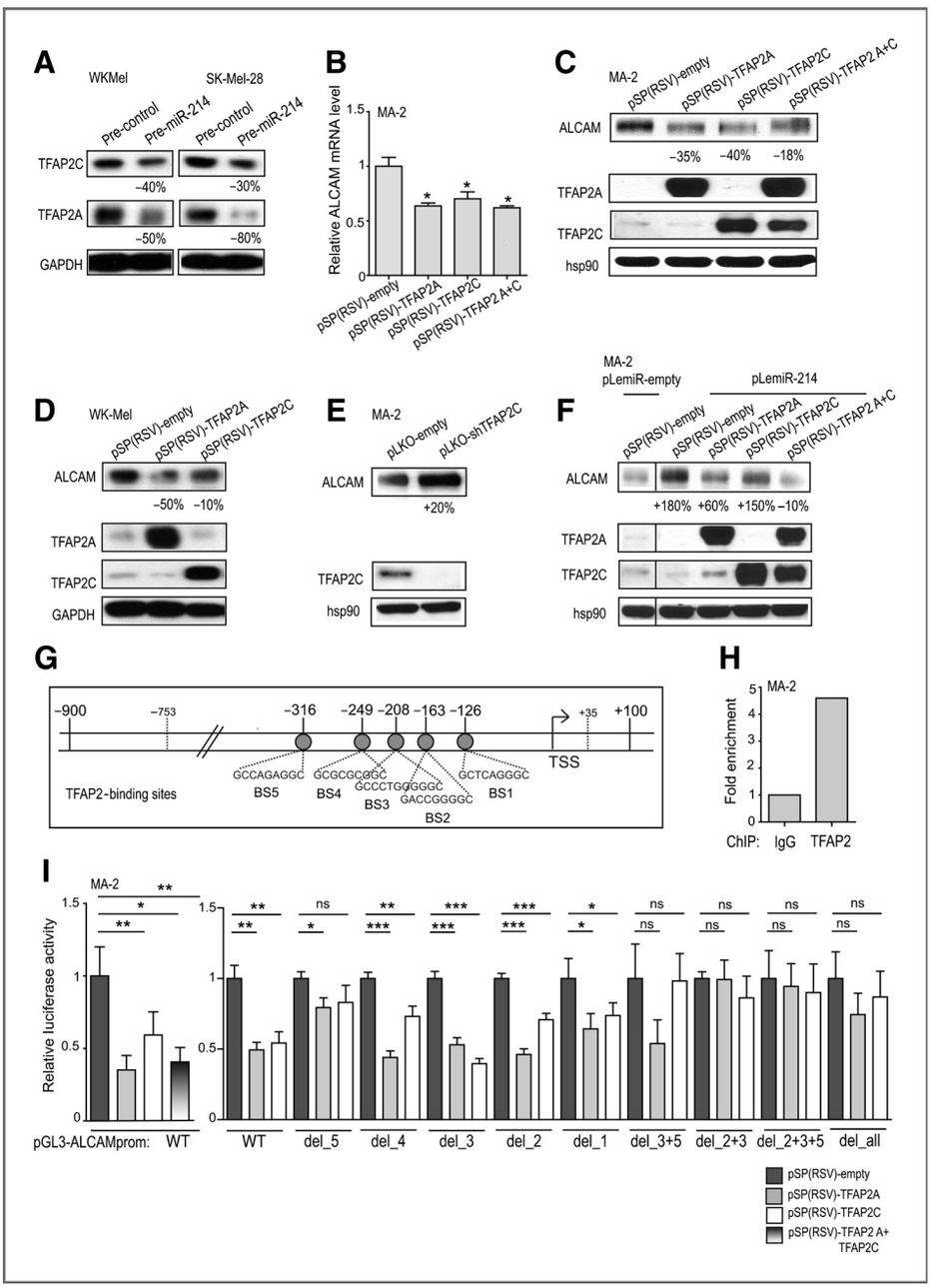

Figure 4. ALCAM is transcriptionally repressed by TFAP2 in melanoma. A–F, ALCAM, TFAP2A, and TFAP2C protein (A, C–F) or mRNA (B) expression levels were analyzed respectively by Western blot analysis and qRT-PCR at 48 (B) and 72 hours (A, C, D, and F) following transient transfection of WK-Mel or SK-Mel-28 with miR-214 precursors or negative controls (pre-miR-214 or -control; A), or of MA-2 or WK-Mel cells (B–D) or of miR-214–overexpressing MA-2 cells (pLemiR-214, F) with pSP(RSV)-empty or TFAP2A or TFAP2C overexpression vectors [pSP(RSV)-TFAP2A or pSP(RSV)-TFAP2C] or the combination of both, or in MA-2 cells stably transduced with either empty or TFAP2C-targeting shRNA vectors (pLKO-empty or pLKO-shTFAP2C, E). In B, results were calculated as fold changes (mean ± SD of triplicates) relative to controls, normalized on 18S RNA level. In A and C–F, protein modulations were calculated relative to controls, normalized on GAPDH or hsp90 loading controls and expressed as percentages. G, scheme showing human *ALCAM* gene promoter region, spanning from −900 to +100 nucleotides around the TSS. Five putative TFAP2-binding sites (BS) are indicated by circles. The portion between −753 and +35 was cloned in pGL3-Basic luciferase reporter vector (pGL3-ALCAMprom; see I). H, ChIP. MA-2 cross-linked sheared chromatin was immunoprecipitated with either negative control (IgG) or anti-TFAP2 antibodies and the TFAP2-binding sites–containing region was PCR-amplified. TFAP2-binding enrichment was calculated relative to IgG-negative control. I, luciferase assays 48 hours posttransfection in MA-2 cells cotransfected with pGL3-Basic reporter constructs containing WT (pGL3-ALCAMprom) or all (del_all) or specific (del_5 to del_1 and del_3+5, 2+3, 2+3+5) TFAP2-binding site-deleted ALCAM promoter sequence cloned upstream of the luciferase coding sequence, together with pSP(RSV)-empty or pSP(RSV)-TFAP2A or pSP(RSV)-TFAP2C expression vectors or the combination of both. Results are shown as mean ± SD of Firefly luciferase activity relative to controls, normalized on *Renilla* luciferase and on the activity measured for the empty pGL3-Basic vector in presence of TFAP2. Two or 3 independent experiments were carried out, in triplicate for B and I and representative results are shown.

transcription start site (TSS), was analyzed with bioinformatics tools, using the canonical TFAP2-binding site PWM consisting of a 9 nucleotide long G/C-rich sequence, shared for TFAP2A and TFAP2C. Five putative TFAP2-binding sites (BS) were identified, with high-affinity binding scores, at positions −316 (BS5), −249 (BS4), −208 (BS3), −163 (BS2), and −126 (BS1; Fig. 4G). A ChIP experiment was carried out using cross-linked MA-2 chromatin, with negative (immunoglobulin G, IgG) or positive (RNA polymerase II, PolII) control or anti-TFAP2 (recognizing both TFAP2A and TFAP2C) antibodies. Importantly, by PCR-amplifying the region containing the 5 TFAP2-binding sites, more than 4-fold TFAP2-binding enrichment was observed on this region relative to IgG-negative control (Fig. 4H). As a positive control PolII-immunoprecipitated DNA was tested with a glyceraldehyde-3-phosphate dehydrogenase (GAPDH) promoter PCR assay (Supplementary Fig. S3A). To test the direct effect of TFAP2 on ALCAM promoter, the activity of the promoter region between −753 and +35 relative to the TSS, was assayed in a luciferase reporter vector (pGL3-ALCAMprom). MA-2 cells were cotransfected with either pGL3-ALCAMprom or pGL3-empty and TFAP2A and/or TFAP2C expression constructs or empty control [pSP(RSV)-TFAP2A, pSP(RSV)-TFAP2C, or pSP (RSV)-empty] and luciferase activity was evaluated 48 hours (Fig. 4I) and 72 hours (Supplementary Fig. S3B) posttransfection. pGL3-ALCAMprom luciferase activity was normalized on pGL3-empty activity in a condition of TFAP2 overexpression. As a positive control, a luciferase construct containing the known TFAP2A-responsive ESDN promoter region (24) was used (Supplementary Fig. S3C). pGL3-ALCAMprom activity was significantly decreased in presence of TFAP2A or TFAP2C or both (60% to 40% reduction), compared with pSP(RSV)-empty control, indicating a direct transcriptional repression of TFAP2 on ALCAM promoter (Fig. 4I, left). The single deletions of the 5 binding sites one-by-one (del_5 to del_1) were not able to rescue the luciferase activity, whereas when we deleted 2 or 3 binding sites in combinations (del_3+5, del_2+3, del_2+3+5) or the entire promoter region included between −316 and −126 thus eliminating all the 5 binding sites (del_all), we were able to abrogate the luciferase activity decrease in presence of TFAP2 (Fig. 4I, right), indicating that the cooperation of the 5 sites is probably required for TFAP2 repression of ALCAM transcription.

miR-214–driven miR-148b downregulation controls ALCAM overexpression posttranscriptionally in melanoma cells

In addition to TFAP2-mediated transcriptional regulation, we considered possible posttranscriptional mechanisms involving other miRs. Because miR-148b was predicted to directly target ALCAM, according to TargetScan 5.2 algorithm (27), we evaluated ALCAM expression following miR-148b overexpression (pre-miR-148b; Supplementary Fig. S1C, S1G, and S1H) compared with pre-control in MA-2, WK-Mel, and SK-Mel-28 cells 72 hours posttransfection. Significantly, a 40% to 80% ALCAM protein reduction was found in Western blot analyses (Fig. 5A–C). To investigate the direct binding of miR-148b on ALCAM, the first 605 bp of ALCAM 3′-UTR (Fig. 5F), containing miR-148b putative binding site (at position 272–277), was cloned in the pMIR-REPORT reporter vector downstream of the luciferase coding sequence (ALCAM3′-UTR). miR-148b–binding site was also mutated (point mutations or deletion; shown in Fig. 5F) to generate mutant ALCAM 3′-UTRs (ALCAMmut and ALCAMdel). Luciferase activity of wild-type (WT) or mutant vectors was evaluated in MA-2 cells in presence or absence of miR-148b overexpression (pre-miR-148b or -control). A significant decrease of luciferase activity was observed for the WT but not for the mutants in presence of miR-148b compared with controls, indicating the specific regulation of miR-148b on ALCAM 3′-UTR (Fig. 5G). As a positive control, a miR-148b sensor construct containing 3 perfect bindings for miR-148b was used (Fig. 5G). Importantly, when we analyzed miR-148b levels in miR-214–overexpressing (pre-miR-214) MA-2, WK-Mel, SK-Mel-28, and MDA-MB-231 cells, a significant reduction of miR-148b expression was found at 24, 48 (Supplementary Fig. S3D; MA-2), and 72 hours (Fig. 5H, MA-2; Fig. 5K, SK-Mel-28; Supplementary Fig. S3E, WK-Mel; Supplementary Fig. S3F, MDA-MB-231 cells) compared with pre-control), as evaluated by qRT-PCR. A similar miR-148b reduction was obtained in stable miR-214–overexpressing (pLemiR-214) MA-2 (Fig. 5I) or WK-Mel (Fig. 5J) cells, compared with empty control (pLemiR-empty). Consistently, miR-148b expression levels were increased in presence of anti-miR-214 in MC-1 cells, compared with anti-control–transfected cells (Fig. 5L). Other unrelated miRs, for instance miR-31, were not affected by miR-214 overexpression (Fig. 5M). These data suggest a regulatory loop between miR-214 and miR-148b, which can affect ALCAM expression. Indeed, the concomitant overexpression of miR-148b and miR-214 (pre-miR-214+pre-miR-148b transfection) in MA-2 cells (Supplementary Fig. S1C) or the reexpression of miR-148b in stable miR-214–overexpressing cells (pLemiR-214+pre-miR-148b; Supplementary Fig. S1D) led to reduced ALCAM protein (Fig. 5A and D) and mRNA (Fig. 5E) levels, similar to control cells (pre-control or pLemiR-empty+pre-control, respectively).

miR-148b downregulation by miR-214 is partially due to TFAP2 control

To explore how miR-214 downregulates miR-148b, we conducted a bioinformatics analysis for miR-148b containing human genomic locus (2,000 nucleotides upstream and downstream of pre-miR-148b), inside the intron 1 of COPZ1 protein-coding gene. First, as described in ref. 28, we used RNA Hybrid algorithm (26) to look for *in silico* evidences of a direct interaction between miR-214 and miR-148b transcript, potentially involved in controlling processing or stability. A single putative 20-nucleotide long miR-214–binding site was found 650 nucleotides downstream of the pre-miR-148b locus (Fig. 6A and B), but with a nonstatistically significant (ns) *P* value (independently of the method used to estimate it, see Materials and Methods and Fig. 6B), leading us to exclude its relevance in this mechanism. Instead, when we looked for putative TFAP2-binding sites in pre-miR-148b–flanking regions, many low- and 3 high-affinity sites were found, including one located 1,816 nucleotides upstream of the pre-miR-148b, having 83% of the maximum PWM score, with a potential role in controlling its

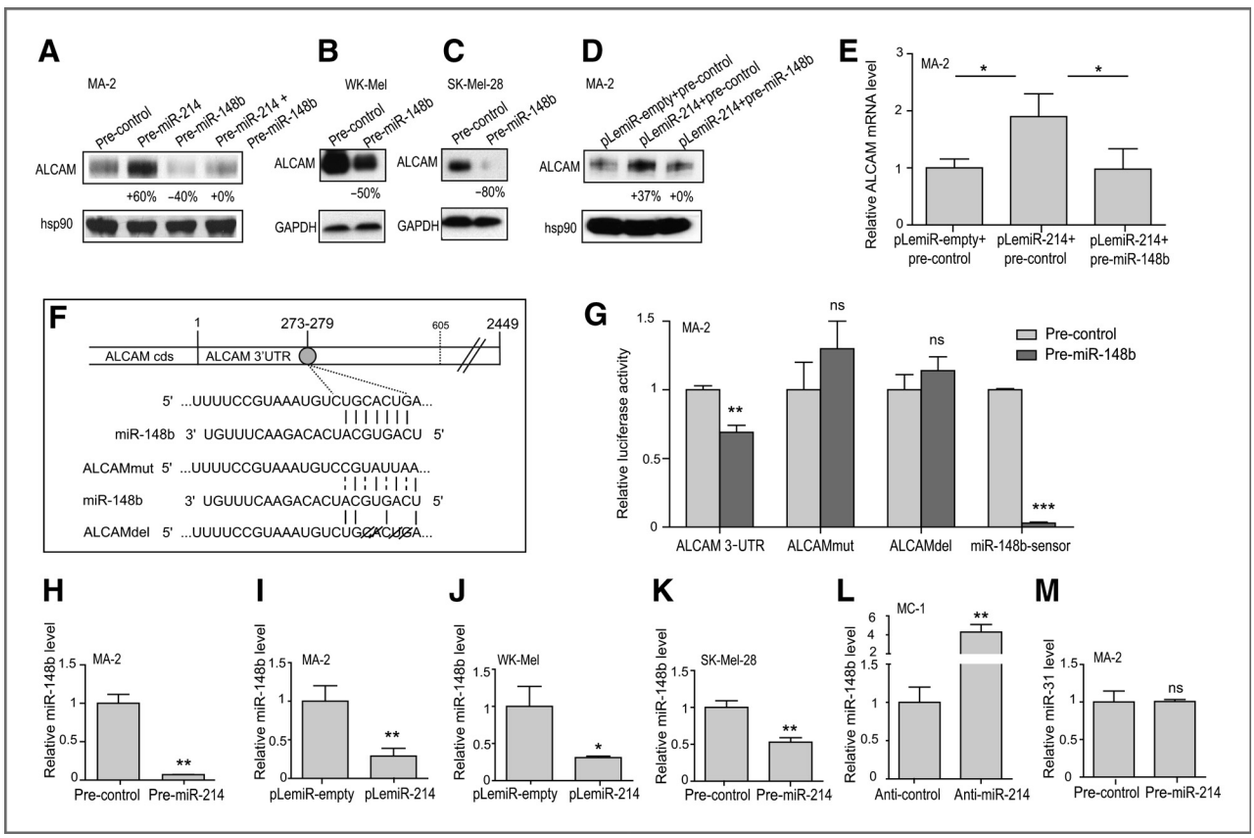

Figure 5. miR-148b directly targets ALCAM and is downregulated by miR-214 in melanoma. A–E, ALCAM protein (A–D) and mRNA (E) expression levels were evaluated by Western blot (A–D) or qRT-PCR (E) analyses, respectively, 48 to 72 hours following transient transfection of MA-2 (A), WK-Mel (B), SK-Mel-28 cells (C), or of miR-214–overexpressing MA-2 cells (pLemiR-214; D and E) with miR-214 and/or miR-148b precursors or negative controls (pre-miR-214 or -148b or -control). Protein modulations were calculated relative to controls, normalized on hsp90 or GAPDH loading controls, and expressed as percentages; mRNA modulations were calculated as fold changes (mean ± SD of triplicates) relative to controls, normalized on 18S RNA level. F, scheme showing WT or mutated (ALCAMmut) or deleted (ALCAMdel) miR-148b–binding site in human ALCAM 3′-UTR (at position 273), paired with miR-148b seed. The portion of ALCAM 3′-UTR cloned in pMIR luciferase reporter vector is up to nucleotide 605, starting from the stop codon. G, luciferase assays in MA-2 cells cotransfected with reporter constructs containing WT (ALCAM3′-UTR) or mutant (ALCAMmut and ALCAMdel) ALCAM 3′-UTRs or a synthetic sequence including 3 perfect miR-148b–binding sites (miR-148b-sensor), cloned downstream of the luciferase coding sequence, together with miR-148b precursors or negative controls (pre-miR-148b or -control). Results are shown as mean ± SD of Firefly luciferase activity relative to controls, normalized on *Renilla* luciferase activity. H–M, miR-148b (H–L) and miR-31 (M) expression levels were tested by qRT-PCR in MA-2 (H, I, and M), WK-Mel (J), SK-Mel-28 (K), or MC-1 (L) cells following transfection with miR-214 precursors (H, K, and M; 72 hours posttransfection) or inhibitors (L; 24 hours posttransfection) or their negative controls (pre- or anti-miR-214 or -control), or transduction with pLemiR-empty or miR-214 overexpression (pLemiR-214) vectors (I and J). Results were calculated as fold changes (mean ± SD of triplicates) relative to controls, normalized on U6 RNA level. Two or 3 independent experiments were carried out in triplicate for E–M and representative results are shown.

transcription (Fig. 6A and C, top). Importantly, as indicated in Fig. 6C, bottom, a ChIP-seq analysis previously conducted on HeLa cells [The ENCODE Project (29), SYDH-TFBS track], revealed TFAP2A and TFAP2C binding in correspondence of this binding site. In line with this, we carried out ChIP experiments in MA-2 cells, as described earlier, and confirmed TFAP2A/C-binding enrichment (1.9-fold) in this region (Fig. 6D), compared with IgG-negative control. These results suggest that the miR-214 regulation on miR-148b is at least partially due to TFAP2-mediated control on miR-148b. Indeed, also miR-148b primary transcript (pri-miR-148b) evaluated by qRT-PCR, was about 30% reduced in miR-214 (pre-miR-214) overexpressing MA-2 cells (Fig. 6E) and, consistently, both pri- (Fig. 6F and G) and mature (Fig. 6H and I) miR-148b levels were more than 50% increased following overexpression of TFAP2A and TFAP2C. Taken together, our data indicate that TFAP2A has a dual role on ALCAM regulation, as summarized in Fig. 6J: it binds on ALCAM promoter and represses ALCAM transcription; it controls ALCAM-targeting miR-148b expression.

miR-148b opposes miR-214–mediated prometastatic functions in melanoma

Because we observed that ALCAM upregulation by miR-214 is at least in part due to miR-148b reduction, we explored the functions of miR-148b in melanoma cell movement. miR-148b was transiently overexpressed in MA-2 and WK-Mel cells by pre-miR-148b transfection and cell migration was evaluated by Transwell assays. Significantly, miR-148b overexpression led to decreased cell movement compared with pre-control (Fig. 7A

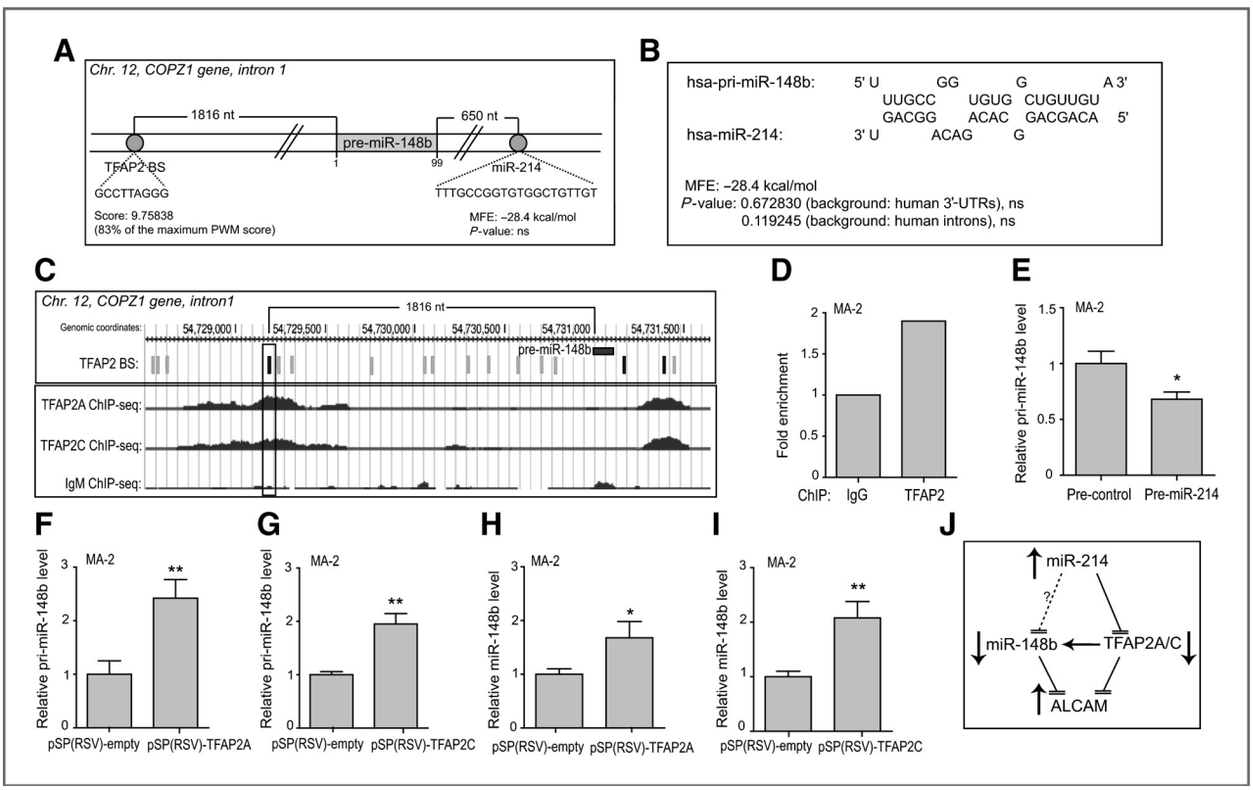

Figure 6. miR-148b downregulation by miR-214 is partially due to a TFAP2-mediated control. A, scheme showing the human pre-miR-148b locus (chromosome 12, intron 1 of COPZ1 protein-coding gene) and the predicted interactions with miR-214 and TFAP2 as shown in B and C. B, referring to A, predicted interaction of miR-214 on the pre-miR-148b locus (650 nucleotides downstream of pre-miR-148b), as obtained with the RNA Hybrid algorithm. MFE, minimum free energy (ΔG) predicted for hybridization; the *P* values were estimated on different backgrounds and are nonstatistically significant (ns). C, referring to A, high affinity (black rectangles; score >80% of the maximum) and low affinity (gray rectangles; score between 60% and 80% of the maximum) TFAP2-binding sites (BS) were obtained by the PWM method (top). The ENCODE Project SYDH-TFBS ChIP-seq analysis conducted on HeLa cells shows TFAP2A and TFAPC but not immunoglobulin M (IgM; negative control) enrichment picks in pre-miR-148b flanking regions, for some putative TFAP2 BS (bottom). D, ChIP. MA-2 cross-linked sheared chromatin was immunoprecipitated with either negative control (IgG) or anti-TFAP2 antibodies and the TFAP2-binding site–containing miR-148b upstream region was PCR-amplified. TFAP2-binding enrichment was calculated relative to IgG-negative control. E–I, miR-148b primary transcript (pri-miR-148b; E–G) and mature miR-148b (H and I) expression levels were tested by qRT-PCR in MA-2 cells 72 hours following transfection with miR-214 precursors or negative controls (pre-miR-214 or -control) or with pSP(RSV)-empty or pSP(RSV)-TFAP2A or pSP (RSV)-TFAP2C expression vectors. Results were calculated as fold changes (mean ± SD of triplicates) relative to controls, normalized on 18S or U6 RNA level. At least 2 independent experiments were carried out in triplicate for E–I and are shown either as representative results (D, F–I) or as the mean ± SEM of 7 independent experiments (E). J, our data show that ALCAM is overexpressed in melanoma because miR-214 downregulates both TFAP2A/C (ALCAM transcriptional repressors) and miR-148b (ALCAM-targeting miR). Relevantly, TFAP2A/C positively regulate miR-148b expression.

and B). Consistently, miR-148b silencing by anti-miR-148b (Supplementary Fig. S1F) resulted in increased cell migration, compared with anti-control–transfected cells (Fig. 7C). More importantly, as shown in Fig. 7D, the concomitant overexpression of miR-148b in miR-214–overexpressing MA-2 cells (pLemiR-214+pre-miR-148b) was able to rescue miR-214–induced increased cell migration (pLemiR-214+pre-control) similarly to control cells (pLemiR-empty+pre-control). We also observed that survival to anoikis was decreased (Supplementary Fig. S3G). We then tested transendothelial migration, as described earlier, and we observed decreased ability of MA-2 cells to migrate through the HUVECs-GFP monolayer when miR-148b was overexpressed (pre-miR-148b) compared with pre-control, opposite to pre-miR-214–transfected cells (Fig. 7E). Remarkably, concomitant miR-148b and miR-214 overexpression (pre-miR-214+pre-miR-148b) completely rescued miR-214–mediated transendothelial migration (Fig. 7E). When we evaluated early lung colonization *in vivo*, 48 hours after tail vein injection of MA-2 cells in nude mice, while miR-214 overexpression (pre-miR-214) significantly enhanced extravasation, miR-148b overexpression alone (pre-miR-148b) moderately reduced it, in comparison with pre-control transfected cells, as shown in Fig. 7F. More importantly, when miR-148b was upregulated in miR-214–overexpressing cells (pre-miR-214+pre-miR-148b), we observed a rescuing of miR-214–induced cell extravasation and early lung colonization (Fig. 7F), suggesting a role for miR-148b in miR-214/ALCAM–mediated melanoma cell metastatic dissemination.

In conclusion, miR-148b is downregulated by miR-214, at least in part via a TFAP2-driven mechanism, and these 2 small RNAs exert opposite roles in melanoma cell dissemination, by controlling ALCAM expression. These observations are strengthened by the analysis of miR-214, miR-148b, ALCAM, and TFAP2 in human patients with melanoma. We took

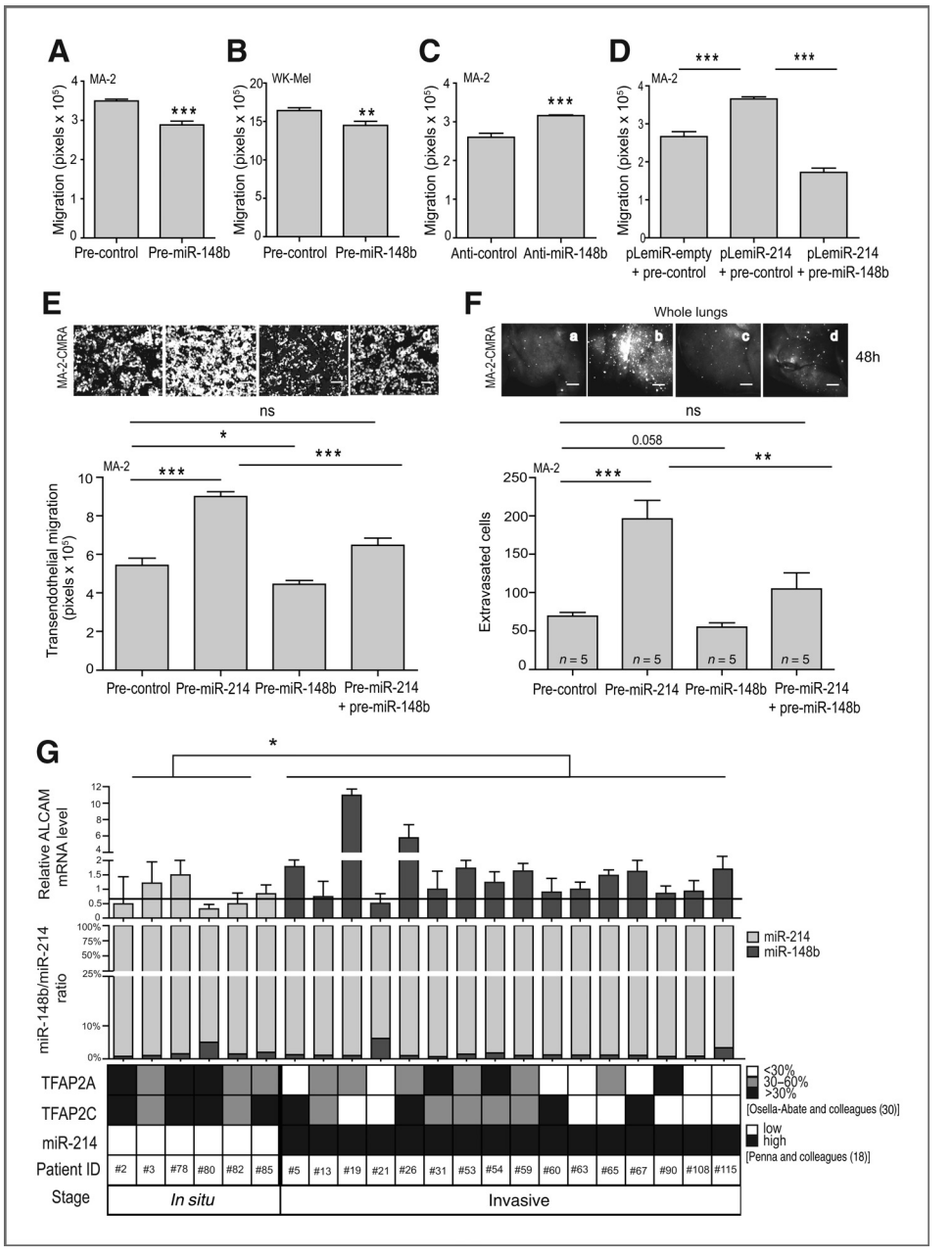

Figure 7. miR-148b opposes miR-214 prometastatic functions in melanoma. A–E, Transwell migration through a pore membrane (A–D) or a fibronectin-coated membrane covered by a confluent monolayer of HUVECs-GFP (E; bar, 50 μm) was evaluated following transient transfection with miR-214 and/or miR-148b precursors or inhibitors or their negative controls (pre-miR-214 or -148b or anti-miR-148b or -control) of MA-2 (A, C, and E; CMRA-labeled in E) or WK-Mel (B) cells or of miR-214–overexpressing MA-2 cells (pLemiR-214; D). F, *in vivo* extravasation assay 48 hours following tail vein injections in nude mice of CMRA-labeled MA-2 cells transfected as in E. Representative pictures of whole lungs are presented (a–d; bar, 800 μm). Results are shown as mean ± SEM of the area covered by migrated cells or of the number of extravasated cells in the lungs, for $n = 5$ mice per group. Two or 3 independent experiments were carried out (in triplicate for A–E) and representative results are shown. G, ALCAM mRNA levels (top) and miR-148b/miR-214 expression ratio (middle) were evaluated in a cohort of $n = 6$ *in situ* versus $n = 16$ invasive human melanomas. Relative protein-coding gene or miR expression was obtained by qRT-PCR analyses, calculated using the median as reference, and normalized on GAPDH or U44 RNA levels, respectively. The horizontal line (top) represents the mean for the *in situ* melanomas. The Mann–Whitney nonparametric test was used for the statistical analysis of ALCAM expression. TFAP2A, TFAP2C, and miR-214 expression levels represented by gray scales (bottom) refer to our previously published works (indicated) and were obtained by immunoistochemical and qRT-PCR analyses, respectively.

advantage of the same cohort of patients used in (18, 30). As indicated in Fig. 7G, bottom, we previously showed that miR-214 was significantly more expressed, whereas TFAP2A and TFAP2C were less expressed, in invasive melanoma samples compared with noninvasive (*in situ*) ones, by qRT-PCR and immunoistochemical analyses, respectively (18, 30). In a

subgroup of the same samples, we now evaluated ALCAM mRNA expression by qRT-PCR and found a significant increase in invasive melanomas ($n = 16$) compared with *in situ* tumors ($n = 6$; Fig. 7G, top), thus reinforcing our findings. Importantly, when we considered miR-148b/miR-214 expression ratio by qRT-PCR in this cohort (Fig. 7G, middle) and in a new independent cohort of patients with melanoma ($n = 10$ *in situ* and $n = 10$ invasive; Supplementary Fig. S4, top), we consistently found low miR-148b (less than 10%) and high miR-214 relative levels, indicating that miR-148b is maintained low in high miR-214–expressing melanomas, at least partially by the earlier described miR-214–mediated mechanism.

Discussion

We previously showed a prometastatic function for miR-214 in melanoma (18). The present work spotted light on the link between miR-214 and ALCAM in the coordination of melanoma progression. Here, we show that ALCAM expression increases when miR-214 is upregulated in several different melanoma cell lines, independently of $BRAF^{V600E}$ mutation status. Previously, we found increased levels of miR-214 in metastatic melanoma cells compared with their poorly malignant counterparts and in invasive or metastatic human melanomas but not in *in situ* samples (18). Supporting the connection between miR-214 and ALCAM are the immunohistochemical analyses for ALCAM in human melanoma samples, which show a perfect correlation between higher levels of ALCAM and thicker lesions or later tumor stages, from common nevi to metastases (8). ALCAM expression was specifically detected at the invasive front of melanomas (8). Moreover, here we highlighted increased ALCAM mRNA expression in invasive high miR-214–expressing human melanomas, compared with *in situ* lesions. In addition, ALCAM resulted to be highly expressed in xenotransplants and metastases originated in mice following injection of melanoma cell variants with high levels of miR-214 (17). Finally, ALCAM expression associates with poor prognosis or relapse for other human tumors, including colorectal, bladder, esophageal, and intraductal breast carcinomas (7, 31, 32) and high ALCAM or miR-214 serum levels are considered poor prognostic markers for some kind of neoplasia (33–36).

ALCAM has a key role in normal tissue or tumor integrity, in heterotypic tumor cell–endothelial cell interactions and in immune cell attachment and transmigration through vessels (5, 6, 37), therefore it is fundamental for primary tumor mass growth and tumor escaping. ALCAM connections are essential for cell movement (9), for efficient conversion of pro-MMP-2 to its active form in metastatic melanoma cells (11) and for the retention of intravascular breast tumor cell clusters in the lung vessels (38). Consistently, we showed that ALCAM overexpression promotes cell migration, whereas silencing blocks it in different melanoma cell lines. More importantly, we proved that miR-214 prometastatic functions are exerted via ALCAM, at least in part. In fact, ALCAM silencing in miR-214–overespressing cells significantly reduces miR-214–mediated increased cell movement, invasion, and transendothelial migration *in vitro* and efficiently impairs extravasation and metastatic dissemination in mice, both following direct injection of melanoma cells in the blood circulation and when we analyzed lung metastatic lesions spontaneously originating from experimental tumors. Because these results were obtained for 3 distinct melanoma cell lines, independently of $BRAF^{V600E}$ mutation status, and for a breast cancer cell line, we conclude that miR-214–mediated ALCAM upregulation has a broad-spectrum key role in tumor cell metastatic dissemination.

Despite the clear correlation between ALCAM expression and melanoma malignancy, the mechanisms leading to ALCAM upregulation are still poorly understood. It is known that ALCAM expression is regulated by promoter CpG islands methylation (38) and by transcriptional regulation exerted by NF-κB (38) and GATA1 (39) transcription factors. Here, we propose that miR-214 regulates ALCAM indirectly via a transcriptional and a posttranscriptional control. About the transcriptional control, we postulate that miR-214 upregulates ALCAM transcription by downregulating its targets TFAP2A and TFAP2C. Loss of TFAP2 during melanoma progression is well documented (40), and we showed here and previously (18) that it is governed, at least in part, by miR-214, in different melanoma cell lines. miR-214 directly targets TFAP2C, whereas TFAP2A is indirectly downregulated, probably via TFAP2C. Indeed, it is known that TFAP2C silencing reduces TFAP2A protein levels (unpublished data) and that TFAP2 family members regulate each other transcriptionally (41). Here, we show that ALCAM mRNA and protein expression decreases in TFAP2-overexpressing MA-2 or WK-Mel cells. Moreover, we identified 5 putative TFAP2-binding sites on ALCAM promoter and proved TFAP2A/C-binding enrichment on this region, via a ChIP experiment. Importantly, we observed a strong downregulation of luciferase expression when the activity of ALCAM promoter was tested in cells overexpressing TFAP2 family members, using a luciferase reporter. The deletion of each single binding site or of combinations of them or of the entire region encompassing the 5 sites suggests their cooperative action. In fact, the ablation of multiple or all sites was able to abrogate TFAP2-dependent luciferase activity reduction. Decreased levels of ALCAM, comparable with low miR-214–expressing cells, were seen in miR-214–overexpressing cells following TFAP2A and, partially, TFAP2C reexpression, indicating that the downmodulation of TFAP2 factors by miR-214, occurring during metastatic dissemination, is necessary to remove the direct transcriptional repression of TFAP2 on ALCAM promoter. Importantly, we previously proved that TFAP2C is responsible for many miR-214 prometastatic functions and that TFAP2C reexpression in miR-214–overexpressing cells was able to rescue miR-214–induced cell movement and early lung metastatic colonization (18). Interestingly, this TFAP2-mediated regulation is similar to what previously shown for the ALCAM homolog MCAM-MUC-18 adhesion molecule in melanoma (42).

About the posttranscriptional control, we showed that miR-214 upregulates ALCAM expression by reducing another small noncoding RNA, miR-148b, which was predicted to directly target ALCAM. In agreement with bioinformatics anticipations, we observed significant downmodulation of ALCAM

protein following miR-148b overexpression. Direct targeting was proven by luciferase reporter assays on WT but not on miR-148b seed-mutants. Importantly, we observed decreased miR-148b levels following miR-214 overexpression in different melanoma cell lines and, *vice versa*, increased levels in miR-214–silenced cells. Significantly, miR-148b overexpression in miR-214–overexpressing cells was able to reestablish low ALCAM levels, as in control cells. Our results suggested a miR-on-miR regulatory loop between miR-148b and miR-214, in which miR-214 could control miR-148b transcription or processing or stability. Another miR-on-miR regulation was previously described for mouse miR-709, which binds on pri-miR-15a/16-1 thus preventing its processing (28). By using the same approach, we looked for possible miR-214 recognition sites around miR-148b locus, but found only a nonstatistically significant putative site, located downstream of pre-miR-148b. Instead, the observation that also pri-miR-148b was down-modulated following miR-214 overexpression and that many putative TFAP2-binding sites were present in miR-148b locus, including a high affinity one in the potential promoter region, led us to investigate a possible transcriptional regulation. On this line, we and others (The ENCODE project) proved TFAP2-binding enrichment on this site by ChIP analyses. In addition, pri- and mature miR-148b expression increased following TFAP2A and TFAP2C overexpression. However, we cannot exclude additional regulations, such as posttranscriptional functions of TFAP2 or, as it is well known that miR-148/152 expression is controlled by promoter methylations (43), possible miR-214–controlled epigenetic mechanisms.

In conclusion, our data indicate that miR-214–driven TFAP2 downregulation occurring during melanoma malignancy, controls ALCAM expression in a dual way: directly, at the transcriptional level, as well as indirectly, by controlling the expression of ALCAM-targeting miR-148b. These data are further reinforced by ours and others observations showing that ALCAM expression increases, whereas TFAP2 decreases and that high levels of miR-214 anticorrelate with poor miR-148b expression during melanoma progression, as assessed in melanoma cell lines and tissues (18, 44). Relevantly, we recently showed that miR-148b inhibits breast cancer progression, mainly by affecting cell movement and survival (45). Similarly, and opposite to what shown for miR-214 (18), miR-148b considerably opposes melanoma cell movement, transendothelial migration and, to a lesser extent, survival to anoikis. More importantly, when miR-148b was upregulated in miR-214–overexpressing cells, it was able to rescue miR-214/ALCAM–mediated prometastatic effects on melanoma cell movement and early lung metastatic colonization.

Taken together, our data indicate that miR-214–driven ALCAM upregulation in metastatic melanoma cells depends on transcriptional (mediated by TFAP2) and posttranscriptional (mediated by miR-148b, itself controlled by TFAP2) mechanisms. Furthermore, miR-214 and miR-148b, with their direct targets, respectively TFAP2 and ALCAM, have opposite effects on melanoma tumor cell dissemination and are part of a new regulatory loop that could be explored for therapeutic attempts.

Disclosure of Potential Conflicts of Interest

No potential conflicts of interest were disclosed.

Authors' Contributions

Conception and design: E. Penna, D. Taverna
Development of methodology: E. Penna, F. Orso
Acquisition of data (provided animals, acquired and managed patients, provided facilities, etc.): E. Penna, F. Orso, D. Cimino, I. Vercellino, E. Quaglino, E. Turco
Analysis and interpretation of data (e.g., statistical analysis, biostatistics, computational analysis): E. Penna, F. Orso, D. Cimino, E. Grassi
Writing, review, and/or revision of the manuscript: E. Penna, D. Taverna
Administrative, technical, or material support (i.e., reporting or organizing data, constructing databases): I. Vercellino, D. Taverna
Study supervision: E. Turco, D. Taverna

Acknowledgments

The authors thank L. Xu, R. Hynes, L. Primo, L. Poliseno, and P. Circosta for providing cell lines, H. Hurst for TFAP2 expression vectors, D. Corà for bioinformatics support, F. Cristofani for providing NSG mice, A. Elia for fluorescence-activated cell sorting (FACS) analyses, M. Forni for microscope photographs, T. Venesio for BRAF mutation analyses, S. Osella-Abate for providing human melanoma samples, R. Coppo for help with mice experiments, A. Perino and A. Camporeale for qRT-PCR technical support.

Grant Support

This work was supported by grants from the Compagnia San Paolo (2008.1054/DT), PRIN 2008/DT, AIRC 2010 (IG10104/DT), and FIRB giovani 2008 (RBFR08F2FS-002/FO). E. Penna is a FIRC fellow (2012–2014).

The costs of publication of this article were defrayed in part by the payment of page charges. This article must therefore be hereby marked *advertisement* in accordance with 18 U.S.C. Section 1734 solely to indicate this fact.

Received September 27, 2012; revised February 26, 2013; accepted March 24, 2013; published OnlineFirst May 10, 2013.

References

1. Parkin DM, Bray F, Ferlay J, Pisani P. Global cancer statistics, 2002. CA Cancer J Clin 2005;55:74–108.
2. Chin L. The genetics of malignant melanoma: lessons from mouse and man. Nat Rev Cancer 2003;3:559–70.
3. Melnikova VO, Bar-Eli M. Transcriptional control of the melanoma malignant phenotype. Cancer Biol Ther 2008;7:997–1003.
4. Bowen MA, Patel DD, Li X, Modrell B, Malacko AR, Wang WC, et al. Cloning, mapping, and characterization of activated leukocyte-cell adhesion molecule (ALCAM), a CD6 ligand. J Exp Med 1995;181:2213–20.
5. Swart GW, Lunter PC, Kilsdonk JW, Kempen LC. Activated leukocyte cell adhesion molecule (ALCAM/CD166): signaling at the divide of melanoma cell clustering and cell migration? Cancer Metastasis Rev 2005;24:223–36.
6. Weidle UH, Eggle D, Klostermann S, Swart GW. ALCAM/CD166: cancer-related issues. Cancer Genomics Proteomics 2010;7:231–43.
7. Ofori-Acquah SF, King JA. Activated leukocyte cell adhesion molecule: a new paradox in cancer. Transl Res 2008;151:122–8.
8. van Kempen LC, van den Oord JJ, van Muijen GN, Weidle UH, Bloemers HP, Swart GW. Activated leukocyte cell adhesion molecule/CD166, a marker of tumor progression in primary malignant melanoma of the skin. Am J Pathol 2000;156:769–74.
9. van Kilsdonk JW, Wilting RH, Bergers M, van Muijen GN, Schalkwijk J, van Kempen LC, et al. Attenuation of melanoma invasion by a secreted variant of activated leukocyte cell adhesion molecule. Cancer Res 2008;68:3671–9.

10. Jannie KM, Stipp CS, Weiner JA. ALCAM regulates motility, invasiveness, and adherens junction formation in uveal melanoma cells. PLoS ONE 2012;7:e39330.
11. Lunter PC, van Kilsdonk JW, van Beek H, Cornelissen IM, Bergers M, Willems PH, et al. Activated leukocyte cell adhesion molecule (ALCAM/CD166/MEMD), a novel actor in invasive growth, controls matrix metalloproteinase activity. Cancer Res 2005;65: 8801–8.
12. Bartel DP. MicroRNAs: target recognition and regulatory functions. Cell 2009;136:215–33.
13. Filipowicz W, Bhattacharyya SN, Sonenberg N. Mechanisms of post-transcriptional regulation by microRNAs: are the answers in sight? Nat Rev Genet 2008;9:102–14.
14. Croce CM. Causes and consequences of microRNA dysregulation in cancer. Nat Rev Genet 2009;10:704–14.
15. Valastyan S, Weinberg RA. MicroRNAs: crucial multi-tasking components in the complex circuitry of tumor metastasis. Cell Cycle 2009; 8:3506–12.
16. Mueller DW, Bosserhoff AK. Role of miRNAs in the progression of malignant melanoma. Br J Cancer 2009;101:551–6.
17. Xu L, Shen SS, Hoshida Y, Subramanian A, Ross K, Brunet JP, et al. Gene expression changes in an animal melanoma model correlate with aggressiveness of human melanoma metastases. Mol Cancer Res 2008;6:760–9.
18. Penna E, Orso F, Cimino D, Tenaglia E, Lembo A, Quaglino E, et al. microRNA-214 contributes to melanoma tumour progression through suppression of TFAP2C. EMBO J 2011;30:1990–2007.
19. Circosta P, Granziero L, Follenzi A, Vigna E, Stella S, Vallario A, et al. T cell receptor (TCR) gene transfer with lentiviral vectors allows efficient redirection of tumor specificity in naive and memory T cells without prior stimulation of endogenous TCR. Hum Gene Ther 2009;20: 1576–88.
20. Primo L, di Blasio L, Roca C, Droetto S, Piva R, Schaffhausen B, et al. Essential role of PDK1 in regulating endothelial cell migration. J Cell Biol 2007;176:1035–47.
21. Poliseno L, Haimovic A, Christos PJ, Vega Y, Saenz de Miera EC, Shapiro R, et al. Deletion of PTENP1 pseudogene in human melanoma. J Invest Dermatol 2011;131:2497–500.
22. Venesio T, Chiorino G, Balsamo A, Zaccagna A, Petti C, Scatolini M, et al. In melanocytic lesions the fraction of BRAF V600E alleles is associated with sun exposure but unrelated to ERK phosphorylation. Mod Pathol 2008;21:716–26.
23. Stormo GD, Fields DS. Specificity, free energy and information content in protein–DNA interactions. Trends Biochem Sci 1998;23:109–13.
24. Orso F, Cora D, Ubezio B, Provero P, Caselle M, Taverna D. Identification of functional TFAP2A and SP1 binding sites in new TFAP2A-modulated genes. BMC Genomics 2010;11:355.
25. Saini HK, Griffiths-Jones S, Enright AJ. Genomic analysis of human microRNA transcripts. Proc Natl Acad Sci U S A 2007; 104:17719–24.
26. Rehmsmeier M, Steffen P, Hochsmann M, Giegerich R. Fast and effective prediction of microRNA/target duplexes. RNA 2004;10: 1507–17.
27. Lewis BP, Burge CB, Bartel DP. Conserved seed pairing, often flanked by adenosines, indicates that thousands of human genes are microRNA targets. Cell 2005;120:15–20.
28. Tang R, Li L, Zhu D, Hou D, Cao T, Gu H, et al. Mouse miRNA-709 directly regulates miRNA-15a/16-1 biogenesis at the posttranscriptional level in the nucleus: evidence for a microRNA hierarchy system. Cell Res 2012;22:504–15.
29. The ENCODE Project Consortium. The ENCODE (ENCyclopedia Of DNA Elements) project. Science 2004;306:636–40.
30. Osella-Abate S, Novelli M, Quaglino P, Orso F, Ubezio B, Tomasini C, et al. Expression of AP-2alpha, AP-2gamma and ESDN in primary melanomas: correlation with histopathological features and potential prognostic value. J Dermatol Sci 2012;68:202–4.
31. Cimino D, Fuso L, Sfiligoi C, Biglia N, Ponzone R, Maggiorotto F, et al. Identification of new genes associated with breast cancer progression by gene expression analysis of predefined sets of neoplastic tissues. Int J Cancer 2008;123:1327–38.
32. Tachezy M, Zander H, Gebauer F, Marx A, Kaifi JT, Izbicki JR, et al. Activated leukocyte cell adhesion molecule (CD166)—its prognostic power for colorectal cancer patients. J Surg Res 2012;177: e15–20.
33. Ihnen M, Kress K, Kersten JF, Kilic E, Choschzick M, Zander H, et al. Relevance of activated leukocyte cell adhesion molecule (ALCAM) in tumor tissue and sera of cervical cancer patients. BMC Cancer 2012;12:140.
34. Witzel I, Schroder C, Muller V, Zander H, Tachezy M, Ihnen M, et al. Detection of activated leukocyte cell adhesion molecule in the serum of breast cancer patients and implications for prognosis. Oncology 2012;82:305–12.
35. Tachezy M, Zander H, Marx AH, Stahl PR, Gebauer F, Izbicki JR, et al. ALCAM (CD166) expression and serum levels in pancreatic cancer. PLoS ONE 2012;7:e39018.
36. Schwarzenbach H, Milde-Langosch K, Steinbach B, Muller V, Pantel K. Diagnostic potential of PTEN-targeting miR-214 in the blood of breast cancer patients. Breast Cancer Res Treat 2012;134: 933–41.
37. Masedunskas A, King JA, Tan F, Cochran R, Stevens T, Sviridov D, et al. Activated leukocyte cell adhesion molecule is a component of the endothelial junction involved in transendothelial monocyte migration. FEBS Lett 2006;580:2637–45.
38. King JA, Tan F, Mbeunkui F, Chambers Z, Cantrell S, Chen H, et al. Mechanisms of transcriptional regulation and prognostic significance of activated leukocyte cell adhesion molecule in cancer. Mol Cancer 2010;9:266.
39. Tan F, Ghosh S, Mbeunkui F, Thomas R, Weiner JA, Ofori-Acquah SF. Essential role for ALCAM gene silencing in megakaryocytic differentiation of K562 cells. BMC Mol Biol 2010;11:91.
40. Bar-Eli M. Gene regulation in melanoma progression by the AP-2 transcription factor. Pigment Cell Res 2001;14:78–85.
41. Bauer R, Imhof A, Pscherer A, Kopp H, Moser M, Seegers S, et al. The genomic structure of the human AP-2 transcription factor. Nucleic Acids Res 1994;22:1413–20.
42. Jean D, Gershenwald JE, Huang S, Luca M, Hudson MJ, Tainsky MA, et al. Loss of AP-2 results in up-regulation of MCAM/MUC18 and an increase in tumor growth and metastasis of human melanoma cells. J Biol Chem 1998;273:16501–8.
43. Lehmann U, Hasemeier B, Christgen M, Müller M, Römermann D, Länger F, et al. Epigenetic inactivation of microRNA gene hsa-mir-9-1 in human breast cancer. J Pathol 2008;214:17–24.
44. Mueller DW, Rehli M, Bosserhoff AK. miRNA expression profiling in melanocytes and melanoma cell lines reveals miRNAs associated with formation and progression of malignant melanoma. J Invest Dermatol 2009;129:1740–51.
45. Cimino D, De Pitta C, Orso F, Zampini M, Casara S, Penna E, et al. miR148b is a major coordinator of breast cancer progression in a relapse-associated microRNA signature by targeting ITGA5, ROCK1, PIK3CA, NRAS, and CSF1. FASEB J 2013;27:1223–35.